Thermodynamic stability of elemental boron allotropes with varying numbers of interstitial atoms

Wataru Hayami [a*], Takanobu Hiroto [b], Kohei Soga [c], Tadashi Ogitsu [d], Kaoru Kimura [e]

[a] Research Center for Materials Nanoarchitectonics, National Institute for Materials Science, Namiki 1-1, Tsukuba, Ibaraki, 305-0044, Japan

[b] Research Network and Facility Services Division, National Institute for Materials Science, Sengen 1-2-1, Tsukuba, Ibaraki, 305-0047, Japan

[c] Department of Medical and Robotic Engineering Design, Tokyo University of Science, Niijuku 6-3-1, Katsushika, Tokyo, 125-8585, Japan

[d] Lawrence Livermore National Laboratory, 7000 East Avenue, Livermore, CA, 94550, USA

[e] Department of Advanced Materials Science, The University of Tokyo, Kashiwanoha 5-1-5, Chiba, 277-8561, Japan

Abstract

Elemental boron exists in multiple allotropes, each characterized by structures containing icosahedral subunits. These structures have interstitial sites between the icosahedral subunits that are partially occupied. The number of atoms in the unit cell varies depending on the occupancy of these interstitial sites. We have investigated the thermodynamic stability of boron allotropes for different numbers of atoms in the unit cell by calculating the free energies, including the contribution of phonons. It has been found that β-rhombohedral boron is most stable with 107 atoms/cell at low temperatures, while it becomes most stable with 105 atoms/cell above 1700 K. This suggests the occurrence of a phase transition at this temperature, which could account for the large variation in the number of atoms in the unit cell for β-rhombohedral boron samples. α-tetragonal boron is consistently most stable with 52 atom/cell and becomes unstable with more than 52 atoms/cell. Similar to β-rhombohedral boron, β-tetragonal boron may undergo a phase transition between 192 and 190 atoms/cell configurations. However, the thermodynamic stability of pure β-tetragonal boron has been questioned in comparison with other allotropes.

Journal of Solid State Chemistry 329 (2024) 124407

https://doi.org/10.1016/j.jssc.2023.124407

* Corresponding author. *E-mail address:* hayami.wataru@nims.go.jp (W. Hayami)

1. Introduction

Boron is an element known to have several allotropes. Rhombohedral forms, α and β (α-rh, β-rh), as well as tetragonal forms, α and β (α-t, β-t), have been recognized since the 1940s [1–5]. γ phase was discovered more recently in 2008 under high pressure [6,7]. Additionally, there are several other reported allotropes that have not yet been sufficiently confirmed [8–11].

Among the confirmed allotropes, β-rh boron is the most stable at ordinary temperature and pressure, and it readily crystalizes from a liquid state. The structural analysis indicates that there are several interstitial sites partially occupied by atoms [12]. Widom et al. proposed the most probable configuration of interstitial atoms in which 107 atoms are included in the unit cell [13]. On the other hand, α-rh boron consists of regularly arranged icosahedral B_{12} units and does not include any interstitial atoms. Despite its simple structure, α-rh boron can be produced in a limited temperature range around 1200°C through methods such as chemical vapor deposition (CVD) [2], platinum flux method [14], or by crystallizing amorphous boron [15].

The history of α-t boron has been controversial. It was first observed in 1943 in a sample produced by CVD [1], and a structural analysis revealed that the tetragonal unit cell included four B_{12} units and two interstitial B atoms [16]. In 1971, however, it was argued that pure α-t boron does not exist stably because it was not synthesized in CVD experiments without the presence of carbon or nitrogen sources [17,18]. In 2003, Wang et al. successfully synthesized α-t boron in the form of nanobelts, which they insisted contained no impurities [19]. The structure of boron nanobelt was analyzed, and the unit cell was found to contain 52.2 atoms [20]. Subsequently, it was theoretically demonstrated that nano-sized α-t boron crystals can exist stably due to their low surface energy [21,22], and the most stable structure of α-t boron was predicted to be B_{52} [23]. In 2016, Ekimov et al. synthesized bulk α-t boron under high pressure starting from decaborane $B_{10}H_{14}$ [24] and confirmed that its structure matched the predicted one [23].

β-t boron was first discovered in 1960 [5] through CVD, and its structure was subsequently analyzed [25]. In 2003, Ma et al. synthesized bulk β-t boron under high-temperature high-pressure conditions [26]. The most stable structure was theoretically predicted to be B_{192} [27].

According to theoretical calculations, boron allotropes, except for γ boron, exhibit very close total energies, differing within a few tens of meV per atom [7,27]. Oganov et al. calculated the free energy of boron allotropes and presented a phase diagram on the pressure-temperature (PT) plane [7]. The diagram showed that β-rh and γ boron were the most stable in low pressure and high pressure regions, respectively. α-rh boron existed in the area between β-rh and γ phases. β-t boron appeared in a high-temperature high-pressure region, while α-t boron never emerged as the most stable state. At the time of their study, the precise configurations of interstitial atoms were still unknown for β-rh, α-t, and β-t boron. Therefore, it is intriguing to investigate how the phase diagram might change when the current knowledge about interstitial atoms is taken into account.

The significance of interstitial atoms becomes evident in certain cases. It has been demonstrated that the configuration of interstitial atoms in β-rh boron leads to geometrical frustration, giving rise to complex physical properties [28,29]. Moreover, there are phenomena that might indicate a phase transition associated with the movement of interstitial atoms, although the underlying mechanism remains uncertain [30–32].

Motivated by the aforementioned observations, our study aims to assess the extent to which interstitial atoms impact the free energies of boron allotropes. We calculate the free energies with varying numbers of atoms in the unit cell, including the entropy of phonons, in order to identify potential phase transitions. By

comparing the free energies on the PT plane, we construct a phase diagram and discuss any deviations from previous findings.

2. Calculation methods

The calculations of the electronic structures and molecular dynamics (MD) simulations were conducted using Quantum ESPRESSO (QE) [33,34], based on the density functional theory with plane waves and pseudopotentials. The ultrasoft pseudopotential [35] of boron was adopted from the library of QE [34]. The generalized gradient approximation functional of Perdew, Burke, and Ernzerhof was employed [36]. An energy cut-off of 50 Ry for plane waves and 350 Ry for electron density was sufficient to provide convergence of the total energy. The total energies were calculated following the optimization of the lattice parameters and the atomic structures at given pressure using Monkhorst-Pack k-point sampling [37] with (8 × 8 × 8), (4 × 4 × 4), (4 × 4 × 8), (4 × 4 × 4), and (4 × 4 × 4) meshes for α-rh, β-rh, α-t, β-t, and γ boron, respectively. The convergence threshold for the forces on atoms was 1.0^{-4} (a.u.). Phonon spectra were calculated with the density-functional perturbation theory using the PHonon package in the QE suite. The q-point grids used to calculate the force constants were (2 × 2 × 2), (1 × 1 × 1), (1 × 1 × 2), (1 × 1 × 1), and (2 × 2 × 2) meshes for α-rh, β-rh, α-t, β-t, and γ boron, respectively. We confirmed that the zero-point phonon energies obtained using these grids were nearly the same as those using finer q-point grids, with an error of 0.54 meV/atom. The contribution of phonons to the free energy was calculated with the quasi harmonic approximation (QHA) [38].

The diffusion coefficients of atoms were determined through MD simulations. The simulations were conducted using a single unit cell for all allotropes. This choice was made because our primary focus was on the movement of interstitial atoms. First, lattice parameters at a specific temperature and pressure were obtained using the Parrinello-Rahman method [39]. Subsequently, MD simulations in the canonical ensemble (NVT) were conducted using the Born-Oppenheimer approximation with a time step of 2.42 fs and a total run time of 4.84 ps. Temperature control was achieved by rescaling the total kinetic energy. The diffusion coefficients were estimated using the Einstein relation [40],

$$D = \frac{1}{2d} \lim_{\tau \to \infty} \frac{d}{d\tau} \langle [r(\tau) - r(0)]^2 \rangle \qquad (1)$$

where D is the diffusion coefficient, d is the dimension of the system, r is the atom's position vector, and τ is time. The angle brackets $\langle\ \rangle$ denote the average over time origins. To be precise, the interstitial atoms in boron crystals would not move randomly but rather follow limited paths when equation (1) may not be applicable. However, in this study, diffusion coefficients are used merely to assess whether or not interstitial atoms migrate; thus the absolute values of diffusion coefficients are not crucial.

3. Results and discussion

The term "interstitial atoms" in this paper refers to atoms that reside in the interstices between icosahedral units with partial occupancy rates. Atoms with a full occupancy rate are denoted as frame atoms. Among boron allotropes, three types, namely β-rh, α-t, and β-t boron have interstitial atoms (Fig. 1). Concerning β-rh, the B13 atom belongs to the (triple) icosahedral unit, but due to its partial occupancy rate [12], it is treated like an interstitial atom in this study. On the other hand, γ boron appears to have interstitial atoms, but they are fully occupied and considered as frame atoms. The notations of interstitial sites for β-rh and β-t are depicted in Fig.

2.

To begin, we examine the case of β-rh boron. Fig. 3 illustrates free energies per atom of β-rh boron calculated within the QHA. The numbers on the graph represent the quantities of atoms in the unit cell, and the free energies are given as relative values compared to the 107-atom cell (black line). For the structures of the 105 to 108-atom cells, we utilized the configurations of interstitial atoms from the work by Widom *et al.* [13], which yielded the lowest total energy excluding the phonon free energy (Table 1). Upon including the phonon contributions, we incidentally discovered that a 107-atom cell with B16 atoms on the *c* and *e* sites (107/B16(*ce*) in Fig. 3) exhibits slightly lower free energy than Widom's lowest-energy model. However, the difference is almost negligible, and we chose Widom's model as the referential free energy. For the remaining structures of the 104 and 109-atom cells, we selected configurations that resulted in the lowest total energy for each atom count.

As temperature increases, the free energies decrease relative to that of the 107-atom cell. This observation is reasonable because the lowest energy structure (107-atom) should exhibit stronger interatomic bondings, resulting in higher phonon energies that generate lower entropy at finite temperatures. Notably, the free energy of the 105-atom cell experiences a significant decrease and becomes lower than that of the 107-atom cell around 1700 K. This suggests that when liquid boron is cooled down, it solidifies into the 105-atom phase at the melting point and then transitions to the 107-atom phase around 1700 K. The mechanism behind the transition from the 105-atom to the 107-atom phase remains unknown, but it is plausible that atoms on the surfaces or grain boundaries diffuse into the bulk and act as interstitial atoms, especially since interstitial atoms can move between sites and cells at temperatures higher than about 700 K [32]. If this view is correct, the phase transition would require adequate time to complete, and when a sample is rapidly cooled down below 700 K, the number of atoms in the cell may not reach 107. This explains why experimental β-rh boron samples have varying numbers of atoms in the unit cell, ranging between 106 and 107 [12].

A similar type of phase transition could also take place in β-t boron. Fig. 4 illustrates the relative free energies of various atom cells of β-t boron, with values relative to that of the 192-atom cell whose structure was adopted from previous work by Hayami [27] (Table 2). The configurations of interstitial atoms for each cell are listed in Table 2, which were chosen to achieve the lowest total energy for each cell. The free energies were calculated at 0 GPa 10 GPa to correspond to the experimental conditions of the synthesis methods, chemical vapor deposition (CVD) [5,25] and high-pressure synthesis [26]. At 0 GPa (Fig. 4 top), the free energy of the 190-atom cell falls below that of the 192-atom cell around 2000 K, suggesting that when a sample is cooled down from a high temperature, the sample undergoes a phase transition from the 190-atom to the 192-atom cell. However, similar to β-rh boron, rapid cooling could disrupt the diffusion of interstitial atoms, resulting in some unit cells not acquiring 192 atoms. This model may explain why a sample produced by CVD had 190 atoms [25]. At 10 GPa (Fig. 4 bottom), the same crossing of the free energies is observed around 2600 K. However, since the melting point of boron at this pressure is estimated to be about 2500 K [41], it remains uncertain whether the phase transition truly occurs. The reports of high-pressure experiments [26] did not specify the atom numbers in the unit cell, providing no clues to judge the occurrence of the phase transition.

Regarding α-t boron, we calculated the free energies at 0 GPa and 10 GPa (Fig. 5 top and bottom) due to its synthesis through two methods, laser ablation [19] and high-pressure synthesis [24]. The values are relative to that of the 52-atom cell, which exhibits the lowest total energy with two interstitial atoms at the 4*c* site (Fig.

1 bottom left) [23]. At 10 GPa, it was discovered that structures with atoms at the 4*c* sites were unstable, while structures with 4*d*-site atoms were stable and exhibited the lowest energy. Consequently, the structures with 4*d*-site atoms are presented for the 10 GPa case (Fig. 5, bottom). At both 0 GPa and 10 GPa, the free energies never descend below that of the 52-atom cell, indicating that the 52-atom cell remains the most stable at all temperatures below the melting point. In terms of experiments, α-t boron nanobelts produced by laser ablation contained 52.2 atoms per cell [20], whereas α-t samples produced by high-pressure synthesis contained 51.6 – 52 atoms [24]. Although there have been limited studies of pure α-t boron, these experiments do not seem to contradict our calculations.

Several observations regarding the structure of α-t boron were incidentally made during the calculations of the free energies. Firstly, it was found that structures with more than 52 atoms per cell proved to be unstable. Although such structures can be optimized under tetragonal or orthorhombic symmetry, they exhibit imaginary phonon modes, indicating structural instabilities. Secondly, the 4*c* sites in α-t boron (Fig. 1) are most favorable for interstitial atoms at 0 GPa [23,24]; however, at 10 GPa, atoms on the 4*c* sites shift toward the 8*h* and 4*d* sites. This observation may elucidate the experimental finding that some interstitial atoms were positioned at the 8*h* sites in α-t boron nanobelts [20].

In the case of γ boron at 0 GPa, the free energy of the 28-atom cell remained lower than that of the 27.5 and 27-atom cells at all temperatures below the melting point. At 30 GPa, the structures of the 27.5 and 27-atom cells were found to be unstable. This indicates that atoms in the interstices between icosahedral units (Fig. 1) play a crucial role in sustaining the γ boron structure and should not be considered as interstitial atoms. This observation aligns with the experimental evidence, indicating that their occupancy rate is nearly 1 [6,7].

Until now, the discussion of free energy has been based on the QHA. However, it is probable that the QHA does not hold at high temperatures for two primary reasons. Firstly, as the amplitude of atomic vibrations increases, higher-order anharmonic terms exert a more significant influence on the vibrations. Secondly, at elevated temperatures, interstitial atoms may begin to hop between neighboring sites, generating configurational entropy and reducing the free energy.

When comparing the free energies, the numbers of frame atoms remain the same among different unit cells for each crystal structure, and it is expected that the effect of anharmonic terms on the frame atoms is largely offset between different cells. The deviation from the QHA is primarily caused by the hopping of interstitial atoms. Based on this assumption, we conducted MD simulations to calculate the diffusion coefficients of interstitial atoms and considered the influence of configurational entropy on the phase transitions that might occur in β-rh (Fig. 3) and β-t boron (Fig. 4).

Fig. 6 presents the diffusion coefficients of atoms in β-rh boron obtained from MD simulations. The temperature was set to 2000 K, slightly above the possible phase transition temperature of 1700 K (Fig. 3). The structures are identical to those used in the free energy calculations, and atoms are indexed indexed by numbers. In the 107-atom cell (Fig. 6 top), the two B16 interstitial atoms (Fig. 1) display significant diffusion coefficients, indicating frequent hopping between neighboring sites, while other atoms exhibit minimal migration. On the other hand, in the case of the 105-atom cell (Fig. 6 bottom), which contains only one B16 interstitial atom, both the B16 atom and an additional B13 atom exhibit substantial migration. Since the number of migrating atoms is the same between the 107- and 105-atom cells, it is expected that the increase in configurational entropy will be nearly identical. Consequently, the deviation from the QHA is almost canceled

between the 107- and 105-atom cells, suggesting that the phase transition between these cells is likely to occur (Fig. 3).

Similarly, we investigated the diffusion coefficients of β-t boron. Figs. 7 and 8 display the diffusion coefficients of the 192- and 190-atom cells at 0 GPa (2000 K) and 10 GPa (2300 K), respectively. At 0 GPa (Fig. 7), the atoms with significant diffusion coefficients are labeled according to atomic sites, totaling 16 atoms for both the 192- and 190-atom cells. While this may be coincidental, it is expected that the migration of atoms would generate the same degree of configurational entropy for the 192- and 190-atom cells. Therefore, the crossing of the free energies of these cells observed in the free energy calculations (Fig. 4 top) may occur. On the other hand, at 10 GPa and 2300 K (Fig. 8), the number of atoms with significant diffusion coefficients is 21 for the 192-atom cell and 15 for the 190-atom cell. As the 192-atom cell contains more diffusive atoms and consequently higher configurational entropy, the crossing of free energy (Fig. 4 bottom) may not occur below the melting point.

Regarding the possible phase transition between the 192- and 190-atom cells, a significant concern arises about the stability of the β-t phase. The diffusion coefficients of β-t boron (Figs. 7 and 8) reveal that several frame atoms (B1–B24p) migrate significantly along with interstitial atoms (B25, B25p, B26), indicating the structural instability of the β-t phase. While this observation might be understandable for 0 GPa since the most stable phase is β-rh, it is unexpected for 10 GPa at 2300 K, where the most stable phase is believed to be β-t [7,26]. The stability of β-t boron will be further discussed later in comparison with other phases (Fig. 9).

In the case of α-t boron, only an interstitial atom at the 4*c* site exhibited migration in the 52-atom cell, while no atoms migrated in the 51-atom cell. Given that the 52-atom cell possesses a larger configurational entropy, the phase transition between the 52- and 51-atom cells would not take place (Fig. 5). The observation that 2*b* atoms hardly migrate confirms their identity as frame atoms, aligning with their full occupancy rates in experiments. The diffusion coefficients of γ boron at 30 GPa and 2000 K indicated that no atoms in the 28-atom cell exhibited migration. Additionally, both the 27- and 27.5-atom cells were unable to sustain the γ boron structure at 30 GPa. Consequently, the two atoms in the interstices (Fig. 1 bottom right) are considered frame atoms.

To construct the phase diagram of boron allotropes, we plotted the relative free energies of α-rh, β-rh (105- and 107-atom), α-t (52-atom), β-t (190- and 192-atom), and γ phases, calculated within QHA, on the PT plane in Fig. 9. These free energies are presented as relative values from that of the β-rh 107-atom cell (light green), where higher values indicate greater stability. Free energies were calculated at 10 GPa intervals within the range of 0 to 30 GPa. These data were then interpolated to generate the free-energy surfaces. The same plot is viewed from both the low-temperature side (Fig. 9 left) and the high-temperature side (Fig. 9 right). The experimental melting point, which is 2370 K at 0 GPa and 2480 K at 7.7 GPa [41], is not considered here.

At 0 GPa and 0 K, the β-rh 107-atom phase (light green) is the most stable. As temperature increases, the β-rh 105-atom phase (dark green) becomes more stable above 1700 K. With increasing pressure at 0 K, the most stable phase transitions as β-rh (107-atom) > α-rh > γ. Additionally, at temperatures above approximately 1800 K, it transitions directly from β-rh (107- or 105-atom) to γ phase. In β-rh boron, the theoretical phase transition between 105- and 107-atom cells occurs up to approximately 7 GPa, beyond which the γ phase becomes more stable than the β-rh phase.

α-t boron is not the most stable phase in any region on the PT plane. Experimentally, pure α-t boron has

been synthesized in a nanobelt form [19]. Studies by Hayami et al. demonstrated that nano-sized α-t boron could be stable due to its low surface energy [21,22]. On the other hand, Ekimove et al. successfully synthesized α-t boron under high pressure using decaborane as a starting material [24], followed by the thermal desorption of residual hydrogen. In this case, α-t boron is considered to be in a metastable state. Other studies claimed to produce α-t boron under conditions similar to those used for β-t boron [8,42,43]. However, in these studies, α-t boron was not obtained as a single phase but rather accompanied by β-rh or γ boron. Therefore, their α-t boron would not be in the most stable state and could possibly include some impurities.

These findings mostly agree with the previous study by Oganov *et al.* [7] except for the appearance of β-rh 105-atom phase. In our study, the β-t phase does not emerge as the most stable state, whereas it does in the previous study within the region around 10–20 GPa, 2000–3000 K. The difference arises because the phase diagram in the previous study was a compilation of computational and experimental results, and the region of β-t boron was estimated from the experiment by Ma *et al.* [26].

When the free energies are examined from the high-temperature side (Fig. 9 right), it is observed that the β-t 192-atom (light blue) and 190-atom (dark blue) phases are close to, but less stable than, the β-rh phase in the pressure range of 0–10 GPa. Considering the deviation from the QHA, it is challenging to definitively determine whether the β-t phase is more or less stable than the β-rh phase. As previously mentioned, the diffusion coefficients of β-t boron (Figs. 7 and 8) suggest its instability in this region. If that is the case, β-t boron synthesized under high pressure [26] and by the CVD method [5,25] might have included a small amount of impurities. This scenario is analogous to the α-t boron case, where impurities such as carbon or nitrogen stabilize the α-t structure [17,18]. It is noteworthy that several other studies [8,9,42,43] did not observe β-t boron under the same conditions as in the experiment by Ma *et al.* [26]. Due to the limited number of reports on β-t boron, additional experiments are required to validate the existence of pure β-t boron.

4. Conclusions

According to the free energies calculated within the QHA, which includes interstitial atoms, β-rh boron undergoes a phase transition between the 107- and 105-atom cells at around 1700 K and 0 GPa. This could explain why β-rh exhibits a large dispersion in atom numbers in the unit cell. However, such a phase transition does not occur in α-t and γ boron. α-t boron is invariably most stable with 52 atoms in the unit cell and becomes unstable with more than 52 atoms. In β-t boron, a similar phase transition might occur between the 192- and 190-atom cells around 2000 K at 0 GPa and 2600 K at 10 GPa. However, the diffusion coefficients calculated by MD simulations show significant migration of frame atoms in β-t boron around the transition temperature, suggesting that β-t boron may not be in a stable state.

Comparing the free energies of all phases on the PT plane, β-rh is the most stable in a low-pressure region, and γ boron is the most stable in a high-pressure region. α-rh boron can exist stably in a region between β-rh and γ boron. On the other hand, α-t boron cannot be the most stable phase in any region. While the difference in free energy between β-t and β-rh boron is small near the melting point at around 10 GPa, β-t boron cannot be deemed the most stable within QHA calculations. Given the substantial migration of frame atoms, pure β-t boron is likely to be unstable and might be stabilized by impurities, similar to what is observed with α-t boron. An experimental study conducted under high temperature and high pressure reported the synthesis of β-t boron, whereas several other studies under similar conditions did not observe it. Therefore, additional experiments

are required to conclusively establish the existence of pure β-t boron.

Acknowledgments

We would like to thank Dr. Satoshi Nakano for valuable discussions. We are also grateful to Prof. Artem R. Oganov for providing helpful information. This work was supported by a MEXT KAKENHI Grant-in-Aid for Scientific Research on Innovative Areas (Grant Numbers JP19H05817, 19H05818, and 19H05819). The calculations in this study were performed on the Numerical Materials Simulator at NIMS. Part of this work was performed under the auspices of the U.S. Department of Energy by Lawrence Livermore National Laboratory under Contract DE-AC52-07NA27344. T.O. is supported by the Computational Materials Sciences Program funded by the US Department of Energy, Office of Science, Basic Energy Sciences, Materials Sciences and Engineering Division.

References

[1] A.W. Laubengayer, D.T. Hurd, A.E. Newkirk, J.L. Hoard, Boron. I. Preparation and properties of pure crystalline boron, J. Am. Chem. Soc. 65 (1943) 1924–1931, https://doi.org/10.1021/ja01250a036.

[2] L.V. McCarty, J.S. Kasper, F.H. Horn, B.F. Decker, A.E. Newkirk, A new crystalline modification of boron, J. Am. Chem. Soc. 80 (1958) 2592, https://doi.org/10.1021/ja01543a066.

[3] D.E. Sands, J. L. Hoard, Rhombohedral elemental boron, J. Am. Chem. Soc. 79 (1957) 5582–5583, https://doi.org/10.1021/ja01577a072.

[4] J.L. Hoard, S. Geller, R.E. Hughes, On the structure of elementary boron, J. Am. Chem. Soc. 73 (1951) 1892–1893, https://doi.org/10.1021/ja01148a555.

[5] C.P. Talley, S. LaPlaca, B. Post, A new polymorph of boron, Acta Crystallogr. 13 (1960) 271–272, https://doi.org/10.1107/S0365110X60000613.

[6] E.Y. Zarechnaya, L. Dubrovinsky, N. Dubrovinskaia, N. Miyajima, Y. Filinchuk, D. Chernyshov, V. Dmitriev, Synthesis of an orthorhombic high pressure boron phase, Sci. Technol. Adv. Mater. 9 (2008) 044209, https://doi.org/10.1088/1468-6996/9/4/044209.

[7] A.R. Oganov, J.H. Chen, C. Gatti, Y.Z. Ma, Y.M. Ma, C.W. Glass, Z.X. Liu, T. Yu, O.O. Kurakevych, V.L. Solozhenko, Ionic high-pressure form of elemental boron, Nature 457 (2009) 863–867, https://doi.org/10.1038/nature07736.

[8] G. Parakhonskiy, N. Dubrovinskaia, E. Bykova, R. Wirth, L. Dubrovinsky, High pressure synthesis and investigation of single crystals of metastable boron phases, High Pressure Res. 33 (2013) 673–683, https://doi.org/10.1080/08957959.2013.806500.

[9] O.O. Kurakevych, V.L. Solozhenko, Crystal structure of dense pseudo-cubic boron allotrope, pc-B52, by powder X ray diffraction, J. Superhard Materials 35 (2013) 60–63, https://doi.org/10.3103/S1063457613010085.

[10] E.V. Podryabinkin, E.V. Tikhonov, A.V. Shapeev, A.R. Oganov, Accelerating crystal structure prediction by machine-learning interatomic potentials with active learning, Phys. Rev. B 99 (2019) 064114, https://doi.org/10.1103/PhysRevB.99.064114.

[11] K.P. Hilleke, T. Ogitsu, S. Zhang, E. Zurek, Structural motifs and bonding in two families of boron structures predicted at megabar pressures, Phys. Rev. Mater. 5 (2021) 053605, https://doi.org/10.1103/PhysRevMaterials.5.053605.

[12] G.A. Slack, C.I. Hejna, M.F. Garbauskas, J.S. Kasper,The crystal structure and density of β-rhombohedral boron, J. Solid State Chem. 76 (1988) 52–63, https://doi.org/10.1016/0022-4596(88)90192-2.

[13] M. Widom, M. Mihalkovič, Symmetry-broken crystal structure of elemental boron at low temperature, Phys. Rev. B 77 (2008) 064113, https://doi.org/10.1103/PhysRevB.77.064113.
[14] F.H. Horn, On the crystallization of simple rhombohedral boron from platinum, J. Electrochem. Soc. 106 (1959) 905–906, https://doi.org/10.1149/1.2427174.
[15] S.O. Shalamberidze, G.I. Kalandadze, D.E. Khulelidze, B.D. Tsurtsumia, Production of α-rhombohedral boron by amorphous boron crystallization, J. Solid State Chem. 154 (2000) 199–203, https://doi.org/10.1006/jssc.2000.8836.
[16] J.L. Hoard, R.E. Hughes, D.E. Sands, The structure of tetragonal boron, J. Am. Chem. Soc. 80 (1958) 4507–4515, https://doi.org/10.1021/ja01550a019.
[17] E. Amberger, K. Ploog, Bildung der gitter des reinen bors, J. Less-Common Met., 23 (1971) 21–31, https://doi.org/10.1016/0022-5088(71)90004-X.
[18] G. Will and K.H. Kossobutzki, X-ray diffraction analysis of $B_{50}C_2$ and $B_{50}N_2$ crystalysing in the "tetragonal" boron lattice, J. Less-Common Met., 47 (1976) 33–38, https://doi.org/10.1016/0022-5088(76)90070-9.
[19] Z. Wang, Y. Shimizu, T. Sasaki, K. Kawaguchi, K. Kimura, N. Koshizaki, Catalyst-free fabrication of single crystalline boron nanobelts by laser ablation, Chem. Phys. Lett. 368 (2003) 663–667, https://doi.org/10.1016/S0009-2614(02)01964-4.
[20] H. Hyodo, Ph. D. Thesis University of Tokyo (2009).
[21] W. Hayami, S. Otani, The role of surface energy in the growth of boron crystals, J. Phys. Chem. C 111 (2007) 688–692, https://doi.org/10.1021/jp065680s.
[22] W. Hayami, S. Otani, Surface energy and growth mechanism of β-tetragonal boron crystal, J. Phys. Chem. C 111 (2007) 10394–10397, https://doi.org/10.1021/jp072594z.
[23] W. Hayami, S. Otani, First-principles study of the crystal and electronic structures of α-tetragonal boron, J. Solid State Chem. 183 (2010) 1521–1528, https://doi.org/10.1016/j.jssc.2010.04.036.
[24] E.A. Ekimov, Y.B. Lebed, N. Uemura, K. Shirai, T.B. Shatalova, V. Sirotinkin, A new orthorhombic boron phase $B_{51.5\text{-}52}$ obtained bydehydrogenation of "α-tetragonal boron", J. Mater. Res. 31 (1916) 2773–2779, https://doi.org/10.1557/jmr.2016.209.
[25] M. Vlasse, R. Naslain, J.S. Kasper, K. Ploog, The crystal structure of tetragonal boron, J. Less-Common Met. 67 (1979) 1–6, https://doi.org/10.1016/0022-5088(79)90067-5.
[26] Y. Ma, C.T. Prewitt, G. Zou, H-k. Mao, R.J. Hemley, High-pressure high-temperature X-ray diffraction of β-boron to 30 GPa, Phys. Rev. B 67 (2003) 174116, https://doi.org/10.1103/PhysRevB.67.174116.
[27] W. Hayami, Structural stability and electronic properties of β-tetragonal boron: A first-principles study, J. Solid State Chem. 221 (2015) 378–383, https://doi.org/10.1016/j.jssc.2014.10.012.
[28] T. Ogitsu, F. Gygi, J. Reed, Y. Motome, E. Schwegler, G. Galli1, Imperfect crystal and unusual semiconductor: Boron, a frustrated element, J. Am. Chem. Soc. 131 (2009) 1903–1909, https://doi.org/10.1021/ja807622w.
[29] T. Ogitsu, F. Gygi, J. Reed, M. Udagawa, Y. Motome, E. Schwegler, G. Galli, Geometrical frustration in an elemental solid: An Ising model to explain the defect structure of β-rhombohedral boron, Phys. Rev. B 81 (2010) 020102(R), https://doi.org/10.1103/PhysRevB.81.020102.
[30] S. Hoffmann, H. Werheit, Phase transition in β-rhombohedral boron near 550 K, Solid State Sci. 14 (2012) 1572–1577, https://doi.org/10.1016/j.solidstatesciences.2012.01.025.
[31] T. Hiroto, K. Soga, K. Kimura, Powder X-ray diffraction study on possible structural change around 550 K in β-rhombohedral boron, Solid State Sci. 104 (2020) 106195, https://doi.org/10.1016/j.solidstatesciences.2020.106195.

[32] T. Hiroto, Y. Morino, M. Yoshikawa, K. Soga, W. Hayami, T. Ogitsu, K. Kimura, Does photoinduced structural change by β-rhombohedral boron occur at room temperature?, Solid State Sci. 142 (2023) 107246, https://doi.org/10.1016/j.solidstatesciences.2023.107246.
[33] P. Giannozzi, O. Andreussi, T. Brumme, O. Bunau, M. Buongiorno Nardelli, M. Calandra, R. Car, C. Cavazzoni, D. Ceresoli, M. Cococcioni, N. Colonna, I. Carnimeo, A. Dal Corso, S. de Gironcoli, P. Delugas, R. A. DiStasio Jr, A. Ferretti, A. Floris, G. Fratesi, G. Fugallo, R. Gebauer, U. Gerstmann, F. Giustino, T. Gorni, J. Jia, M. Kawamura, H. Y. Ko, A. Kokalj, E. Küçükbenli, M. Lazzeri, M. Marsili, N. Marzari, F. Mauri, N. L. Nguyen, H. V. Nguyen, A. Otero-de-la-Roza, L. Paulatto, S. Poncé, D. Rocca, R. Sabatini, B. Santra, M. Schlipf, A. P. Seitsonen, A. Smogunov, I. Timrov, T. Thonhauser, P. Umari, N. Vast, X. Wu and S. Baroni, Advanced capabilities for materials modelling with Quantum ESPRESSO, J. Phys.: Condens. Matter, 29 (2017) 465901, https://doi.org/10.1088/1361-648X/aa8f79.
[34] Quantum ESPRESSO, http://www.quantum-espresso.org.
[35] D. Vanderbilt, Soft self-consistent pseudopotentials in a generalized eigenvalue formalism, Phys. Rev. B, 41 (1990) 7892–7895, https://doi.org/10.1103/PhysRevB.41.7892.
[36] J.P. Perdew, K. Burke, M. Ernzerhof, Generalized gradient approximation made simple, Phys. Rev. Lett. 77 (1996) 3865–3868, https://doi.org/10.1103/PhysRevLett.77.3865.
[37] H.J. Monkhorst, J.D. Pack, Special points for Brillouin-zone integrations, Phys. Rev. B 13 (1976) 5188–5192, https://doi.org/10.1103/PhysRevB.13.5188.
[38] M.T. Dove, *Introduction to lattice dynamics*, Cambridge university press (1993), https://doi.org/10.1017/CBO9780511619885.
[39] M. Parrinello and A. Rahman, Crystal structure and pair potentials: A molecular-dynamics study, Phys. Rev. Lett. 45 (1980) 1196–1199, https://doi.org/10.1103/PhysRevLett.45.1196.
[40] G. Pranami, M.H. Lamm, Estimating error in diffusion coefficients derived from molecular dynamics simulations, J. Chem. Theory Comput. 11 (2015) 4586–4592, https://doi.org/10.1021/acs.jctc.5b00574.
[41] V.V. Brazhkin, T. Taniguichi, M. Akaishi, S.V. Popova, Fabrication of β-boron by chemical-reaction and melt-quenching methods at high pressures, J. Mater. Res. 19 (2004) 1643–1647, https://doi.org/10.1557/JMR.2004.0224.
[42] J. Qin, T. Irifune, H. Dekura, H. Ohfuji, N. Nishiyama, L. Lei, T. Shinmei, Phase relations in boron at pressures up to 18 GPa and temperatures up to 2200°C, Phys. Rev. B 85 (2012) 014107, https://doi.org/10.1103/PhysRevB.85.014107.
[43] O.O. Kurakevych, Y. Godec, T. Hammouda, C. Goujon, Comparison of solid-state crystallization of boron polymorphs at ambient and high pressures, High Pressure Res. 32 (2012) 30–38, https://doi.org/10.1080/08957959.2011.635145.

Table 1. Configurations of interstitial atoms for β-rh boron. The notation of interstitial sites (*a* – *f*) for B13, B16, B17, and B18 is depicted in Fig. 2 (left), following the work by Widom *et al.* [13]. 107* represents the configuration of 107/B16(*ce*) in Fig. 3.

Number of atoms /unit cell	Configuration
104	B13(*bcef*) B16(*a*)
105	B13(*bcdef*) B16(*a*)
106	B13(*bcdef*) B16(*bd*)
107	B13(*bcef*) B16(*bd*) B17(*a*) B18(*a*)
107*	B13(*bcef*) B16(*ce*) B17(*a*) B18(*a*)
108	B13(*bcef*) B16(*acd*) B17(*a*) B18(*a*)
109	B13(*bcef*) B16(*acef*) B17(*a*) B18(*a*)

Table 2. Configurations of interstitial atoms for β-t boron. The notation of interstitial sites (1 – 4) for B25, B25p, and B26 is depicted in Fig. 2 (right), following the work by Hayami *et al.* [27].

Number of atoms /unit cell	Configuration
184	B25(-) B25p(-) B26(-)
186	B25(13) B25p(-) B26(-)
188	B25(1234) B25p(-) B26(-)
190	B25(1234) B25p(-) B26(12)
191	B25(-) B25p(1234) B26(123)
192	B25(-) B25p(1234) B26(1234)
193	B25(1) B25p(1234) B26(1234)
194	B25(13) B25p(1234) B26(1234)
196	B25(1234) B25p(1234) B26(1234)

Figures and captions

Fig. 1. Structures of β-rh, α-t, β-t, and γ boron. Green icosahedra represent B_{12} units, and blue polyhedra correspond to a triple and a double icosahedron for β-rh and β-t boron, respectively. Interstitial sites are labeled.

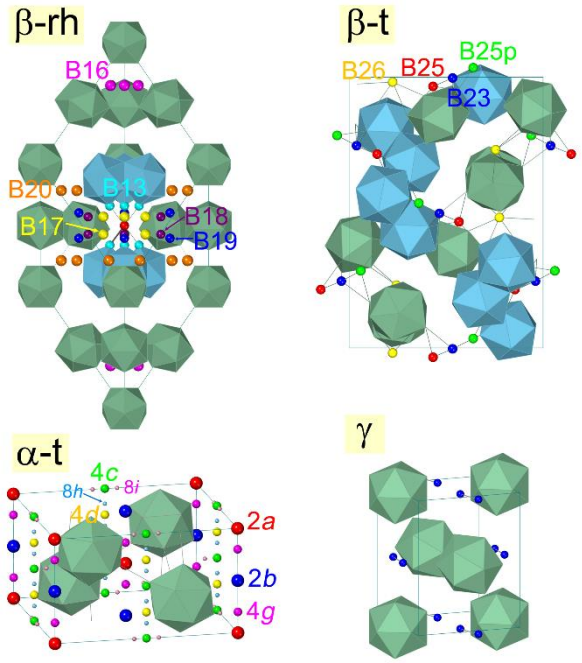

Fig. 2. Notations of interstitial sites used in Tables 1 and 2. On the left, β-rh boron viewed from the [111] direction; on the right, β-t boron viewed from the [001] direction.

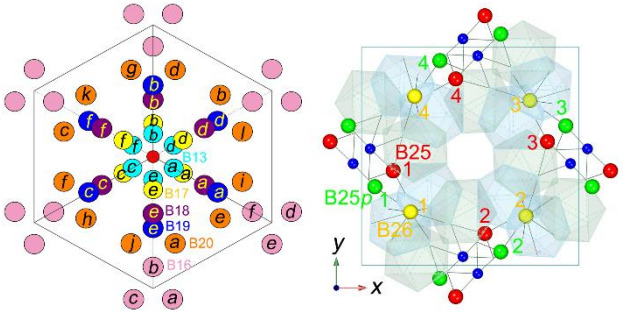

Fig. 3. Relative free energies of β-rh boron at 0 GPa. The numbers on curves indicate the number of atoms in the unit cell. Free energies are relative to that of the 107-atom cell (black line).

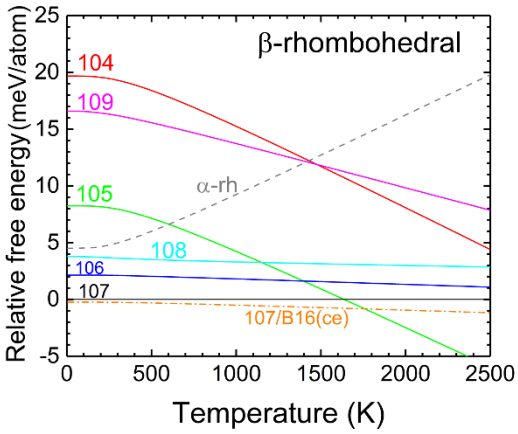

Fig. 4. Relative free energies of β-t boron at 0 and 10 GPa. Free energies are relative to that of the 192-atom cell (black line).

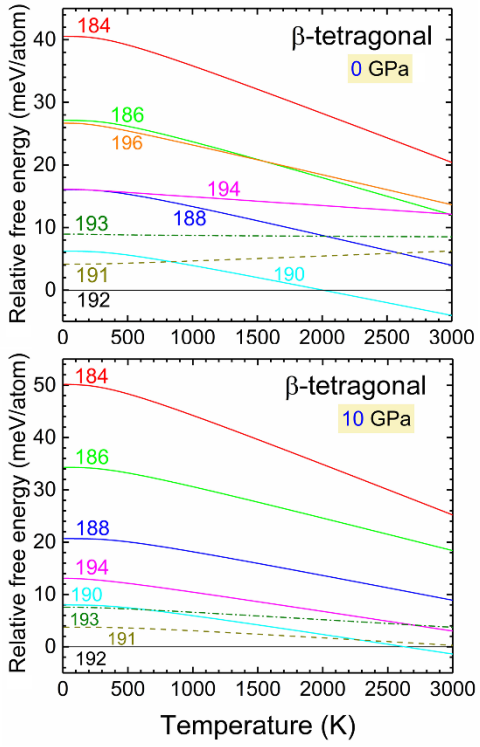

Fig. 5. Relative free energies of α-t boron at 0 and 10 GPa. Free energies are relative to that of the 52-atom cell (black line). At 10 GPa, interstitial atoms shift from the 4*c* sites to the 4*d* sites.

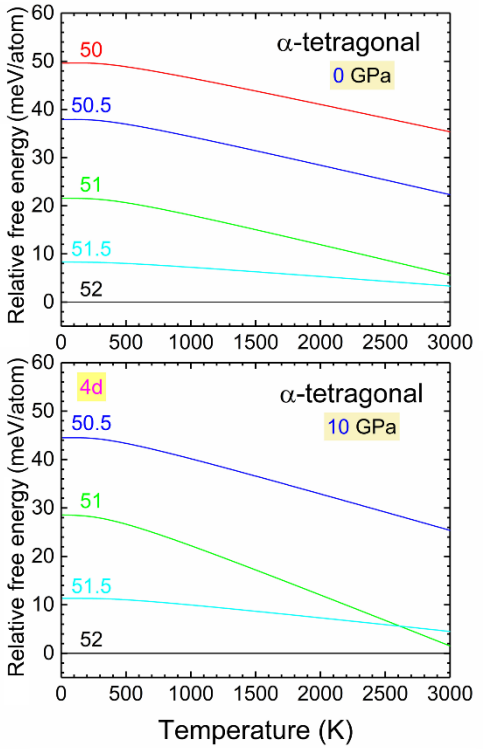

Fig. 6. Diffusion coefficients of the 107- and 105-atom cells of β-rh boron. The original positions of B13 and B15 atoms are indicated in Fig. 1.

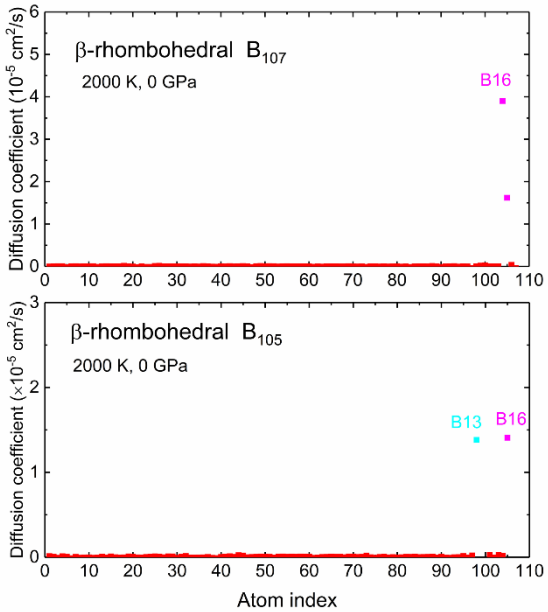

Fig. 7. Diffusion coefficients of the 192- and 190-atom cells of β-t boron at 0 GPa. Atoms other than B23, B25, B25p and B26 are frame atoms not explicitly indicated in Fig. 1.

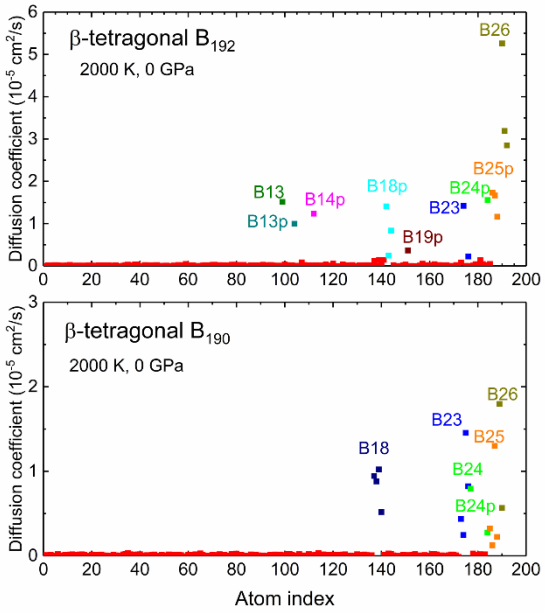

Fig. 8. Diffusion coefficients of the 192- and 190-atom cells of β-t boron at 10 GPa. Atom labels are the same as in Fig. 7.

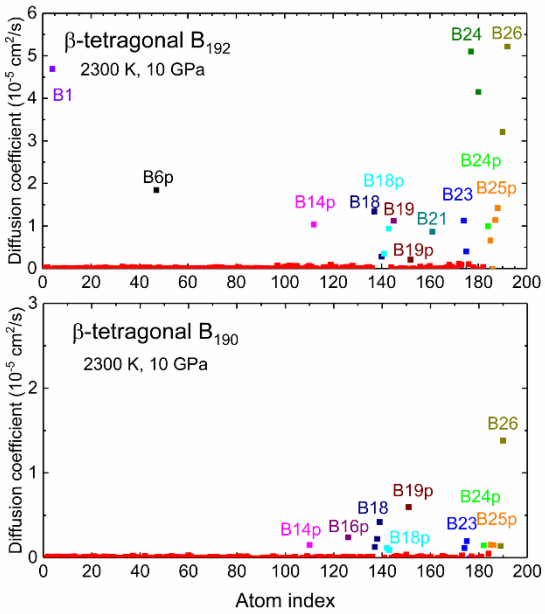

Fig. 9. Relative free energies of boron allotropes plotted on the PT plane. Free energies are relative values from that of the 107-atom cell of β-rh boron (light green plane). The same graph is viewed from the low-temperature side (left) and the high-temperature side (right).